Dispersal scaling from the world's rivers

Jonathan A. Warrick[1] and Derek A. Fong[2]

Received 19 November 2003; accepted 15 January 2004; published 19 February 2004.

[1] Although rivers provide important biogeochemical inputs to oceans, there are currently no descriptive or predictive relationships of the spatial scales of these river influences. Our combined satellite, laboratory, field and modeling results show that the coastal dispersal areas of small, mountainous rivers exhibit remarkable self-similar scaling relationships over many orders of magnitude. River plume areas scale with source drainage area to a power significantly less than one (average = 0.65), and this power relationship decreases significantly with distance offshore of the river mouth. Observations of plumes from large rivers reveal that this scaling continues over six orders of magnitude of river drainage basin areas. This suggests that the cumulative area of coastal influence for many of the smallest rivers of the world is greater than that of single rivers of equal watershed size. *INDEX TERMS:* 4235 Oceanography: General: Estuarine processes; 4528 Oceanography: Physical: Fronts and jets; 1899 Hydrology: General or miscellaneous. **Citation:** Warrick, J. A., and D. A. Fong (2004), Dispersal scaling from the world's rivers, *Geophys. Res. Lett.*, *31*, L04301, doi:10.1029/2003GL019114.

1. Introduction

[2] Rivers are important sources of dissolved and particulate fluxes to the world's oceans [*Martin and Whitfield*, 1983], and a disproportionate amount of this flux is derived from small, mountainous rivers [*Milliman and Syvitski*, 1992; *Carey et al.*, 2002]. Dispersal patterns of river discharge (Figure 1a) directly influence many biogeochemical systems, such as coastal sediment budgets [*Wheatcroft et al.*, 1997], carbon export to oceans [*Raymond and Cole*, 2003], nutrient export and phytoplankton blooms [*Smith and Hitchcock*, 1994], pollution dispersal [*Bay et al.*, 1999] and habitat functioning [*McCulloch et al.*, 2003]. Research of ocean dispersal from the important small, mountainous rivers, however, is confounded by the shear number (tens of 1000s) and variability (e.g., watershed sizes range 10 to >10,000 km^2) of sites to be investigated. Unfortunately, discharge dispersal from these small, mountainous rivers is less well understood than dispersal from the largest rivers of the world, such as the Amazon [*Geyer et al.*, 1996] and the Mississippi [*Walker*, 1996].

[3] Recent studies suggest that flood events are important to the total fluxes from small, mountainous rivers [*Wheatcroft et al.*, 1997; *Warrick and Milliman*, 2003], and that river plumes during these events are initially dominated by river inertia due to high discharge velocities [*Geyer et al.*, 2000]. This water dispersal will occur within thin (1–10 m) but extensive (1–1000's of km^2) hypopycnal (i.e., positively buoyant) river plumes, which spread along the ocean water surface, and are important pathways for dissolved and particulate materials.

[4] Since rivers exhibit self-similar scaling patterns over both geomorphic and hydrologic properties [*Rodriguez-Iturbe and Rinaldo*, 1997], a first-order assumption is that power law relationships are applicable to river dispersal from a relatively uniform geomorphic and hydrologic region. This is to say that river plume area (P), watershed area (A), and the number of plumes (N) with areas greater than i would be related over several orders of magnitude by:

$$P = c A^b \tag{1a}$$

$$N_i = a P^{-\beta} \tag{1b}$$

where a, b, c, and β are regionally-based, or perhaps universal, constants. Here we investigate the applicability of Equation 1 to small, mountainous river plumes using remote sensing, scaling relationships from field and laboratory investigations, and numerical modeling.

2. Remote Sensing

[5] Remote sensing analyses of river plumes can be used to provide synoptic assessments of dispersal relationships. Since discharge rates from large rivers of a region may not be temporally coherent [e.g., *Salisbury et al.*, 2001], we only use imagery from small flooding rivers, which have received coherent and intense pulses of rainfall. We cannot, however, control for river plumes that may have significantly different sediment grain size distributions or rates of flocculation, although we assume that these factors have limited importance within the semi-continuous geomorphic regions we present here [see *Mertes and Warrick*, 2001 for discussion].

[6] A remotely sensed image of extensive plumes off Morocco was obtained by the NASA MODIS system aboard the Aqua satellite in November 26, 2002 immediately following intensive flooding (Figure 1a). Plumes in this image were delineated by the extent of turbidity fronts, which include spectral characteristics of suspended sediment, dissolved materials and phytoplankton. We assumed that plumes advected only offshore and poleward of the river mouths (the apparent direction of ambient currents). The plumes from the Oued Nefifikh and Oued Mellah drainages (labeled 6 and 7) could not be easily distinguished due to cloud cover, so the total combined plume area is partitioned equally between these rivers. Even though the Oued Sabou plume (labeled 1) is not shown in its entirety in Figure 1a, the total plume area for it is represented in Figure 1b. Using

[1]Coastal and Marine Geology, United States Geological Survey, Menlo Park, California, USA.
[2]Environmental Fluid Mechanics Laboratory, Department of Civil and Environmental Engineering, Stanford University, Stanford, California, USA.

0094-8276/04/2003GL019114$05.00

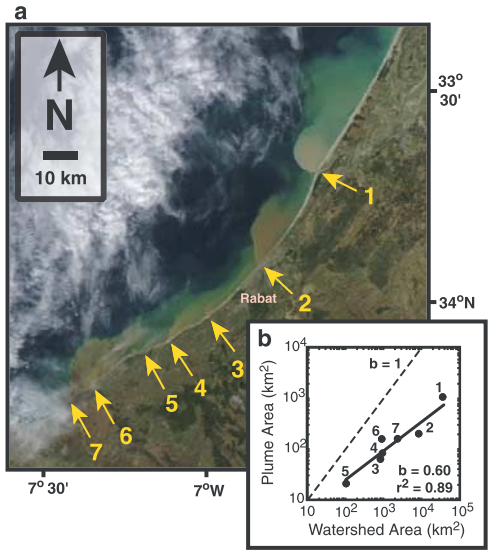

Figure 1. River plumes from flooding Moroccan rivers on 26 November 2002, as recorded by MODIS. (a) True-color representation of plumes. Seven river mouths are identified with yellow arrows (1 – Oued Sebou, 2 – Oued Bou Regreg, 3 – Oued Yquem, 4 – Oued Cherrat, 5 – unnamed, small drainage, 6 – Oued Nefifikh, and 7 – Oued Mellah). A portion of the Oued Sabou plume extends north of the figure boundary. (b) The relationship between watershed drainage area and river plume area.

this methodology, plume areas range from 21 to 1100 km^2 (Figure 1b). When compared to river drainage area, these plume areas produce a power law slope (b; Equation 1a) significantly less than one (0.60 ± 0.09, $r^2 = 0.89$; Figure 1b).

[7] Previously reported remote sensing observations of river suspended sediment plumes along 1300-km of the California coast [*Mertes and Warrick*, 2001] varied between 1 and 230 km^2 in area (Figure 2a); and plume dispersal area and watershed area exhibit a power relationship (Equation 1a) in which $b = 0.63 \pm 0.15$ ($r^2 = 0.63$). Scatter about this relationship is likely due to the combined local effects of discharge variability and environmental forcing on the plumes, since the residuals are not related to geologic province or geographic region.

[8] Although there is scatter in the plume size-watershed size relationship, the California plumes show a remarkable power law size-frequency relationship throughout two orders of magnitude of plume sizes ($\beta = 1.02 \pm 0.03$; Figure 2b). Since this power law scale is indistinguishable from 1, the observed cumulative plume area is equally distributed between all plume sizes. The relationship between cumulative plume area and cumulative watershed area is shown in Figure 2c; 50% of the cumulative plume area is attributed to less than 20% of the cumulative watershed area (representing the smallest rivers of this region). These data closely match theoretical plume relationships (shown with solid and dashed lines; Figure 2c) computed with Equation 1a and watershed river size-frequency data from *Leopold et al.* [1964].

3. Scaling Relationships

[9] Previous laboratory investigations of buoyant plumes [*Fischer et al.*, 1979] can also be used to elucidate plume scales. This work shows that plume dispersal patterns are largely a function of fluid fluxes of mass, momentum and buoyancy. In these studies, the plume is described in terms of a mass flux length scale (l_Q), which characterizes the region of flow establishment near the river mouth, and a momentum length scale (l_M), which characterizes the offshore transition point between momentum and buoyancy dominated forcing. Plume areas associated with these length

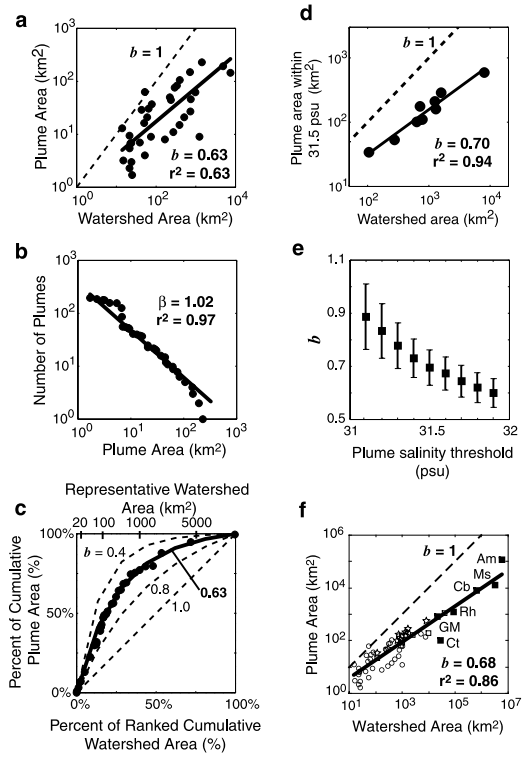

Figure 2. River plume relationships derived from satellite remote sensing, numerical modeling and shipboard observations. (a–c) Relationships from analyses of SeaWiFS remote sensing for coastal California watersheds on February 9, 1998 [after *Mertes and Warrick*, 2001]. (a) The relationship between watershed area and plume area. (b) Size-frequency relationships of the California river plumes. (c) Cumulative river plume area from the cumulative coastal California watershed ranked by watershed area (filled circles). Also shown are theoretical plume area-watershed area relationships for four values of b (lines), where the size-frequency relationship of source watersheds was obtained from Table 5-2 of *Leopold et al.* [1964]. (d, e) River plume numerical model results. (d) Maximum river plume area as constrained by 31.5 psu salinity threshold. (e) The relationship between plume salinity threshold and power law slope, b. (f) Maximum plume areas following exceptional events from larger rivers of the world (filled squares) along with results shown previously in Figures 1b (unfilled squares), 2a (unfilled circles) and 2d (unfilled stars). Large rivers include: Amazon (Am), Mississippi (Ms), Columbia (Cb), Rhone (Rh), Gulf of Maine (GM), and Connecticut (Ct), which were obtained from *Geyer et al.* [2000], *Walker* [1996], *Hickey et al.* [1998], *Marsaleix et al.* [1998], *Stumpf and Goldschmidt* [1992], and *Garvine* [1974].

scales ($P_Q \sim l_Q^2$ and $P_M \sim l_M^2$) have been found to be related to river discharge characteristics:

$$P_Q = Q\,V^{-1} \tag{2a}$$

$$P_M = Q^{1/2}\,V^{3/2}(g')^{-1} \tag{2b}$$

where Q is river discharge, V is average river velocity, and g' is the buoyancy anomaly of river water as compared to ocean water [*Fischer et al.*, 1979].

[10] Within a relatively continuous geomorphic and hydrologic region, Q and V can be related to watershed area, A, using discharge scaling relationships. Since flood dispersal is a function of peak discharge rates [*Geyer et al.*, 2000], Q is proportional to approximately $A^{0.85}$ as shown by flood recurrence intervals due to probabilities of spatially coincident precipitation, structure of stream channel networks, and flood wave attenuation [*Dunne and Leopold*, 1978]. Using Manning's equation, V is proportional to $R^{2/3}$, $S^{1/2}$ and n^{-1}, where R is the hydraulic radius (river cross sectional area divided by the wetted perimeter), S is the channel slope, and n is the channel roughness [*Chow*, 1959]. These parameters will vary with increasing river size (in general, R will increase, while S and n will decrease). However, these effects typically negate each other so that V is proportional to A^C where C is between -0.1 and 0.1 [*Dunne and Leopold*, 1978]. Hence, assuming g' is constant regionally, P_Q and P_M are proportional to approximately $A^{0.85}$ and $A^{0.43}$, respectively. Thus, b is predicted to be considerably less than 1, consistent with the remote sensing results presented above. Also note that b for the inshore, mass flux scale (P_Q) is twice the offshore, momentum scale (P_M), which suggests an inverse relationship between b and distance from the river mouth.

4. Numerical Modeling

[11] Finally, numerical modeling can be used to further evaluate scaling patterns of river plumes. We utilize *Blumberg and Mellor*'s [1987] ECOM-3D primitive equation hydrodynamic model, which has been used in several previous studies of river plumes [e.g., *Garvine*, 1999; *Fong and Geyer*, 2002]. ECOM-3D employs the *Mellor and Yamada* [1982] Level 2.5 turbulence closure model to parameterize vertical mixing and *Smagorinky*'s [1963] horizontal mixing scheme. In addition, a recursive *Smolarkiewicz and Grabowski* [1990] method is used to advect the scalar fields, minimizing the effects of numerical diffusion. For simplicity, the influence of tides, winds, and ambient currents are neglected and the river discharges are perpendicular to the coast. While these variables are certainly important in river plume dynamics [see *Morehead and Syvitski*, 1999; *Horner et al.*, 2000; *Fong and Geyer*, 2001; *Yankovsky et al.*, 2001; *Fong and Geyer*, 2002], they are neglected in this study in order to ascertain the first-order scaling relationships associated with the buoyancy forcing.

[12] ECOM-3D is used to calculate plume areas for river boundary conditions as parameterized by discharge variables (peak and total event discharge, stream depth, and stream width) from nine northern California rivers, which have the fundamental size relationships that exist in rivers throughout the world (see Supplementary Data[1]). Plume areas for each modeled river-event are calculated using salinity thresholds (calculated for 0.1 psu intervals from the ambient ocean 32 psu) to define the plume boundary.

[13] Maximum plume areas for each modeled river-event closely follow the power law patterns of Equation 1a (e.g., b for the 31.5 psu salinity threshold is 0.70 ± 0.07; Figure 2d). Values of b are inversely related to the salinity threshold used to define the plumes (Figure 2e), which suggests that b decreases with distance offshore (since plume areas often equal zero for thresholds approaching 31 psu and lower, thresholds lower than 31 psu are not considered).

5. Discussion/Conclusions

[14] Results from the three methods suggest that the first-order scaling of small, mountainous river plumes exhibit self-similar patterns, and b (Equation 1a) is substantially less than unity. A value of $b < 1$ implies that the combined smallest rivers spread their materials over a much larger area than a single river of the same drainage area (e.g., Figure 2c). These patterns largely arise due to the efficiency of flood peak generation in small watersheds, which imparts higher rates of river mass and momentum flux per unit watershed area. Since watershed characteristics are known to be fractal globally [*Rodriguez-Iturbe and Rinaldo*, 1997] we predict that these patterns are applicable to small, mountainous rivers worldwide.

[15] These patterns continue throughout the larger rivers of the world (Figure 2f), as shown by the greatest observed plumes from a number of these systems (comparable to 5–100 year recurrence interval floods). However, the power law exponent of these results ($b = 0.68 \pm 0.04$) is likely high due to differences in event recurrence. Nevertheless, this suggests global patterns of river plumes follow the size relationships described above, even though dispersal forcing mechanisms may be fundamentally different across these systems [*Garvine*, 1995].

[16] The spatial and temporal scales of river biogeochemical impacts are related to rates of alteration, uptake, dispersion, and settling of the various constituents within these river plumes. For example, sediment particles have distinct settling properties that remove sediment mass from river plumes, while dissolved constituents (including nutrients), remain in plumes until biologic uptake or other transformations occur, typically much farther offshore [e.g., *Smith and Hitchcock*, 1994]. We therefore hypothesize that biogeochemical processes will result in different scaling relationships (Equations 1a and 1b) for each plume constituent, in part because b appears to decrease with plume distance offshore. For many constituents, however, not only do small, mountainous rivers output significantly higher yields [*Milliman and Syvitski*, 1992; *Carey et al.*, 2002], but these rivers also disperse materials of interest over cumulatively larger areas than larger rivers of the same watershed size.

[17] River plumes are complicated dynamical systems subject to several different oceanographic forcings and hydraulic controls near the river mouth. Additionally, as noted above, the details of the sedimentation and biological

[1] Auxiliary material is available at ftp://ftp.agu.org/apend/gl/2003GL019114.

dynamics will be relevant to gain additional insight into satellite imagery as well as information on the fate of constituents of interest. Continued work is needed to evaluate these and other controls on river plumes and constituent transport that are locally and regionally important to the fundamental self-similar scaling relationships shown here.

[18] **Acknowledgments.** We are grateful for the insightful reviews of Richard Garvine and James Syvitski. Tom Parsons, David Rubin and Alex Horner provided careful reviews on an earlier draft of the manuscript, and John D. Milliman and Scott Peckham participated in early discussions regarding these topics. JAW was supported by a USGS Mendenhall Postdoctoral Fellowship. DAF acknowledges the Office of Naval Research for support and Alan Blumberg for permission to use ECOM-3D.

References

Bay, S. M., B. H. Jones, and K. C. Schiff (1999), Study of the impact of stormwater discharge on Santa Monica Bay, report, 16 p., Southern California Coastal Water Research Project, Westiminster, Calif.

Blumberg, A. F., and G. L. Mellor (1987), A description of a three-dimensional coastal ocean circulation model, in *Three-dimensional Coastal Ocean Models*, edited by N. Heaps, pp. 1–16, AGU, Washington D.C.

Carey, A. E., et al. (2002), Trace metal fluxes to the ocean: The importance of high-standing oceanic islands, *Geophys. Res. Lett.*, *29*(23), 2099, doi:10.1029/2002GL015690.

Chow, V. T. (1959), *Open-Channel Hydraulics*, 680 pp., McGraw-Hill, New York.

Dunne, T., and L. B. Leopold (1978), *Water in environmental planning*, 818 pp., W. H. Freeman, San Francisco.

Fischer, H. B., E. J. List, R. C. Y. Koh, J. Imberger, and N. H. Brooks (1979), *Mixing in Inland and Coastal Waters*, 482 pp., Academic, San Diego.

Fong, D. A., and W. R. Geyer (2001), The response of a river plume during an upwelling favorable wind event, *J. Geophys. Res.*, *106*(C1), 1067–1084.

Fong, D. A., and W. R. Geyer (2002), The alongshore transport of freshwater in a surface-trapped river plume, *J. Phys. Oceanography*, *32*, 957–972.

Garvine, R. W. (1974), Physical features of the Connecticut River outflow during high discharge, *J. Geophys. Res.*, *79*, 831–846.

Garvine, R. W. (1995), A dynamical system for classifying buoyant coastal discharges, *Cont. Shelf Res.*, *15*, 1585–1600.

Garvine, R. W. (1999), Penetration of buoyant coastal discharge onto the continental shelf: A numerical model experiment, *J. Phys. Oceanogr.*, *29*, 1892–1909.

Geyer, W. R., et al. (1996), Physical oceanography of the Amazon shelf, *Cont. Shelf Res.*, *16*, 575–616.

Geyer, W. R., P. Hill, T. Milligan, and P. Traykovski (2000), The structure of the Eel River plume during floods, *Cont. Shelf Res.*, *20*, 2067–2093.

Hickey, B. M., L. J. Pietrafesa, D. A. Jay, and W. C. Boicourt (1998), The Columbia River plume study: Subtidal variability in the velocity and salinity fields, *J. Geophys. Res.*, *103*(CC5), 10,339–10,368.

Horner, A. R., D. A. Fong, J. R. Koseff, T. Maxworthy, and S. G. Monismith (2000), The control of coastal current transport. 5th International Symposium on Stratified Flows, *International Association of Hydraulic Research*, *2*, 865–870.

Leopold, L. B., M. G. Wolman, and J. P. Miller (1964), *Fluvial Processes in Geomorphology*, 522 pp., Dover Publications, New York.

Marsaleix, P., C. Estournel, V. Kondrachoff, and R. Vehil (1998), A numerical study of the formation of the Rhone River plume, *J. Marine Sys.*, *14*, 99–115.

Martin, J.-M., and M. Whitfield (1983), The significance of the river input of chemical elements to the ocean, in *Trace Metals in Sea Water*, edited by C. S. Wong, E. A. Boyle, K. W. Bruland, J. D. Burton, and E. D. Goldberg, pp. 265–296, Plenum Press, New York.

McCulloch, M., et al. (2003), Coral record of increased sediment flux to the inner Great Barrier Reef since European settlement, *Nature*, *421*, 727–730.

Mellor, G. L., and T. Yamada (1982), Development of a turbulence closure model for geophysical fluid problems, *Rev. Geophys.*, *20*, 851–875.

Mertes, L. A. K., and J. A. Warrick (2001), Measuring flood output from 110 coastal watersheds in California with field measurements and SeaWiFS, *Geology*, *29*, 659–662.

Milliman, J. D., and J. P. M. Syvitski (1992), Geomorphic/tectonic control of sediment discharge to the ocean: The importance of small mountainous rivers, *J. Geol.*, *100*, 525–544.

Morehead, M. D., and J. P. M. Syvitski (1999), River plume sedimentation modeling for sequence stratigraphy: Application to the Eel Shelf, California, *Mar. Geol.*, *154*, 29–41.

Raymond, P. A., and J. J. Cole (2003), Increase in the export of alkalinity from North America's largest river, *Science*, *301*, 88–91.

Rodriguez-Iturbe, I., and A. Rinaldo (1997), *Fractal River Basins, Chance and Self-Organization*, 547 pp., Cambridge Univ. Press, Cambridge.

Salisbury, J. E., J. W. Campbell, L. D. Meeker, and C. Vörösmarty (2001), Ocean color and river data reveal fluvial influence in coastal waters, *Eos*, *82*(20), 226–227.

Smagorinsky, J. (1963), General circulation experiments with the primitive equations, 1. the basic experiment, *Monthly Weather Rev.*, *91*, 99–164.

Smith, S. M., and G. L. Hitchcock (1994), Nutrient enrichments and phytoplankton growth in the surface waters of the Louisiana bight, *Estuaries*, *17*, 740–753.

Smolarkiewicz, P. K., and W. W. Grabowski (1990), The multi-dimensional positive definite advection transport algorithm, *J. Computational Physics*, *86*, 355–375.

Stumpf, R. P., and P. M. Goldschmidt (1992), Remote sensing of suspended sediment discharge into the western Gulf of Maine during the April 1987 100-year flood, *J. Coastal Res.*, *8*, 218–225.

Walker, N. D. (1996), Satellite assessment of Mississippi River plume variability: Causes and predictability, *Remote Sens. Env.*, *58*, 21–35.

Warrick, J. A., and J. D. Milliman (2003), Hyperpycnal sediment discharge from semiarid southern California rivers: Implications for coastal sediment budgets, *Geology*, *31*, 781–784.

Wheatcroft, R. A., C. K. Sommerfield, D. E. Drake, J. C. Borgeld, and C. A. Nittrouer (1997), Rapid and widespread dispersal of flood sediment on the northern California margin, *Geology*, *25*, 163–166.

Yankovsky, A. E., B. M. Hickey, and A. Munchow (2001), The impact of variable inflow on the dynamics of a coastal buoyant plume, *J. Geophys. Res.*, *106*(C9), 19,809–19,824.

J. A. Warrick, Coastal and Marine Geology, United States Geological Survey, 345 Middlefield Rd., MS 999, Menlo Park, CA 94025-3591, USA. (jwarrick@usgs.gov)

D. A. Fong, Environmental Fluid Mechanics Laboratory, Department of Civil and Environmental Engineering, Stanford University, Stanford, CA 94305-4020, USA.